XXVI CREEM
Congresso Nacional de Estudantes de Engenharia Mecânica
ILHÉUS/ITABUNA - BAHIA

ABCM
Associação Brasileira de Engenharia e Ciências Mecânicas

XXVI Congresso Nacional de Estudantes de Engenharia Mecânica,
CREEM 2019
19 a 23 de agosto de 2019, Ilhéus, BA, Brasil

VIBRATION SUPPRESSION ON A ROTATING MACHINE BY THE USE OF ELECTROMAGNETIC ACTUATORS AND A PID CONTROLLER

Iago Alves Pereira, iago.pereira@ufu.br
Leandro de Souza Leão, leao@ufu.br
Felipe do Carmo Carvalho, fcc@ufu.br
Aldemir Aparecido Cavalini Junior, aacjunior@ufu.br
Valder Steffen Junior, vsteffen@ufu.br
LMEst – Structural Mechanics Laboratory, Federal University of Uberlândia, School of Mechanical Engineering, Av. João Naves de Ávila, 2121, Uberlândia, MG, 38408-196, Brazil

Abstract. *Vibration will always be present in rotating machines and its amplitudes are especially due to unbalance forces. However, due to safety reasons and design constraints, vibration levels should be kept as small as possible. This way, this paper presents an electromagnetic actuator (EMA) to be applied on a rotating machine on its bearing position, composing a hybrid bearing, aiming at shaft vibration suppression. A proportional-integral-derivative (PID) controller will be used for deriving the desired control laws. A rotor composed by a flexible horizontal shaft, two rigid discs, and two self-aligning ball bearings is modeled by the so-called finite elements (FE) method, considering the Timoshenko beam theory. The numerical results are encouraging, highlighting the efficiency of the PID technique to control vibrations on rotating machines.*

Keywords: *rotating machines, vibration suppression, PID controller, finite elements method*

1. INTRODUCTION

Vibration in rotating machines are undesired, but also unavoidable. They cause the rotating machine to degrade much faster, besides generating efficiency losses. Balancing methods are useful, but they need to be performed again every time any machine feature is modified, even for the simple variation of its rotating speed.

In this sense, vibration control methods are much more interesting, for their versatility. Vibration control counts with passive and active methods. The passive methods are usually designed for specific operation conditions. They usually consist on varying some dynamic characteristic of the rotor, such as mass, stiffness or damping, according to Steffen-Jr *et al.* (2000). The system is tuned for reaching a new dynamic behavior on a specific operation range. On the other hand, active control methods are capable of adapting themselves, according to the machine requirements on different conditions.

For this reason, this paper deals with an active PID controller, for absorbing the vibrations of a horizontal rotor. As just stated, this controller may adapt itself for different necessities of the machine. However this first study is devoted for controlling shaft vibrations only at constant speeds. New papers will be written as this study progresses, showing all the PID capabilities. Some PID theory may be encountered at the reference Ogata (2010).

Many other active controllers may be found on the literature, such as linear quadratic regulator (LQR) Koroishi *et al.* (2015), H_∞ synthesis Nair *et al.* (2009) or fuzzy logic Cavalini-Jr *et al.* (2015). Although these techniques are very powerful, their design is much more complex. Therefore, one may say that a PID controller represents an interesting option, since it derives good results compared to the other mentioned techniques, but presents very simple concepts.

2. METHODOLOGY

2.1 Numerical FE Model

According to Lallane and Ferraris (1997), a rotating machine may be represented by Eq. 1:

$$\mathbf{M}\ddot{\mathbf{q}} + [\mathbf{D} + \Omega\mathbf{D}_g]\,\dot{\mathbf{q}} + \mathbf{K}\mathbf{q} = \mathbf{W} + \mathbf{F}_u + k\mathbf{F}_{EMA} + \Delta\mathbf{K}\mathbf{q} \tag{1}$$

where $\mathbf{M}$ stands for the mass matrix, $\mathbf{D}$ for the damping matrix, $\mathbf{D}_g$ for the gyroscopic effect and $\mathbf{K}$ for the stiffness matrix. All of these matrices are related to moving parts of the rotating machine, such as disks, couplings and shaft. The generalized coordinate vector is represented by $\mathbf{q}$ and the rotating speed, by Ω. On the right hand side of Eq.1, the forces are presented, such as $\mathbf{W}$, for the weight force, $\mathbf{F}_u$ for the unbalance forces, $\mathbf{F}_{EMA}$ for the electromagnetic actuators forces and $\Delta\mathbf{K}\mathbf{q}$ for the crack force, which is considered to be concentrated only in the cracked element. Finally, the parameter k will represent the controller gain, responsible to decrease rotor vibration amplitudes.

This differential equation was solved by using the numerical FE method, which was built for representing the real test rig presented in Fig. 1(a). The FE mesh, composed by 31 elements is used to mathematically characterize the system and is depicted in Fig. 1(b).

Figure 1: Test rig used for crack control: (a) real test rig; (b) mesh for the FE model

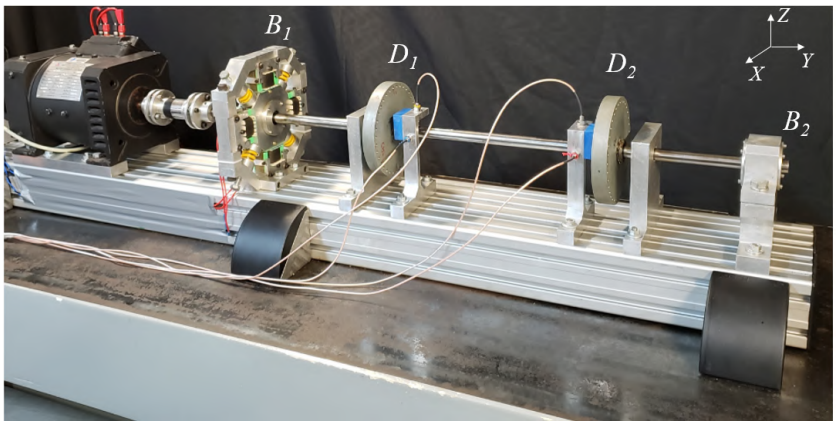

(a)

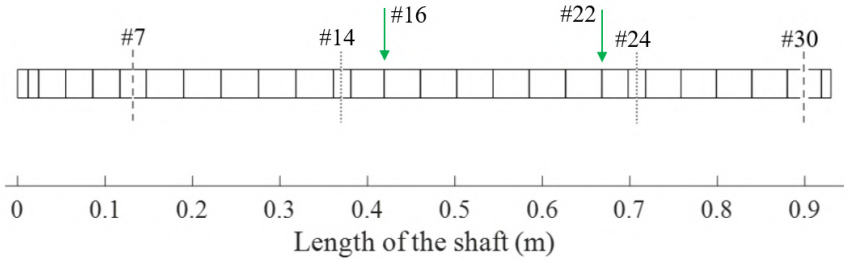

(b)

The rotating machine is composed by a flexible steel shaft with 930 mm length and 17 mm diameter ($E = 182\ GPa$, $\rho = 7930\ kg/m^3$, $\nu = 0.29$), two rigid discs D_1 (node $\#14$; $2.599\ kg$) and D_2 (node $\#24$; $2.587\ kg$), both of steel, and two roller bearings (B_1 and B_2, located at the nodes $\#7$ and $\#30$, respectively). In this machine, displacement sensors are orthogonally mounted on the nodes $\#16$ (S_{16_X} and S_{16_Z}) and $\#22$ (S_{22_X} and S_{22_Z}) to collect the shaft vibration.

2.2 Model Updating

After building the numerical model, it is necessary to check if its responses are close to the ones of the real test rig. Usually an adjust between both responses is necessary. At this paper, a model updating procedure was performed to determine the unknown parameters of the rotor FE model, namely the stiffness coefficients k of the bearings, the modal damping ξ_i of the six first vibration modes ($i = 1, \ldots, 6$), and the angular stiffness k_{ROT} due to the coupling between the electric motor and the shaft (added around the orthogonal directions X and Z of the nodes $\#1$ and $\#2$; see Fig. 1(b)).

In this work, the Differential Evolution optimization technique was used in the model updating procedure, accordint to Cavalini-Jr *et al.* (2016); Storn and Price (1995). The experimental FRFs were obtained on the test rig with the shaft at rest. A hammer was used to apply impact forces along the X and Z directions of both discs, separately. The response signals were measured by the two proximity probes (i.e., S_{16} and S_{22}) positioned along the same direction of the impacts resulting 8 FRFs.

The measurements were performed by using the dynamic analyzer Agilent® (model 35670A) in a range of 0 to 100 Hz in steps of 0.25 Hz. Table 1 summarizes the parameters determined in the end of the minimization process.

Figure 2 compares the simulated and experimental FRF obtained from impacts along the horizontal direction of D_1 and the sensor $S16_X$. Note that the FRF generated from the FE model is satisfactorily close to the one obtained directly from the test rig. Similar results were obtained for the remaining FRFs.

Figure 3 presents the first four vibration modes of the rotor system, associated with the following natural frequencies: 24.56 Hz, 25.10 Hz, 74.70 Hz, and 79.22 Hz, respectively.

The numerical Campbell diagram of the rotating machine considered in this paper is shown in Fig. 4, having its first and second backward and forward critical speeds are printed on it.

Table 1: Design space of the optimization problem k $[N/m]$, ξ [dimensionless] and $k_{t_{coup}}$ $[Nm/rad]$

Parameters	Values	Parameters	Values
$k_{X_{B_1}}$	$8.55x10^5$	ξ_1	0.009
$k_{Z_{B_1}}$	$5.203x10^7$	ξ_2	0.099
$k_{X_{B_2}}$	$1.198x10^6$	ξ_3	0.009
$k_{Z_{B_2}}$	$7.023x10^8$	ξ_4	0.030
k_{ROT}	554.5		

Figure 2: Comparison between numerical and experimental frequency responses

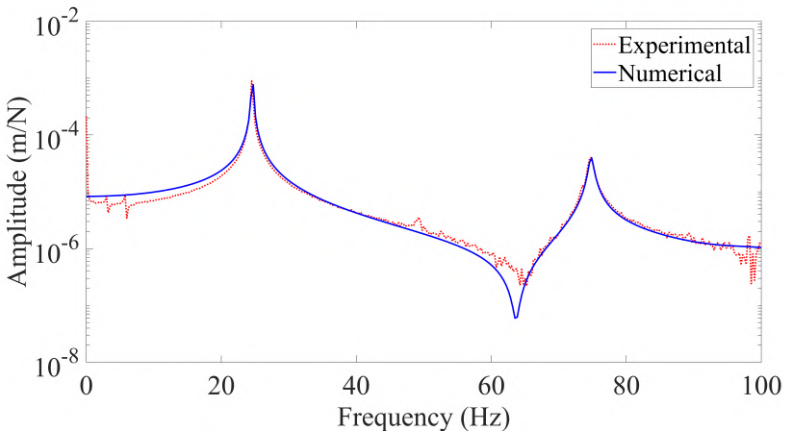

Figure 3: Rotor first (—) and second (—) mode shapes: (a) X horizontal direction; (b) Z vertical direction

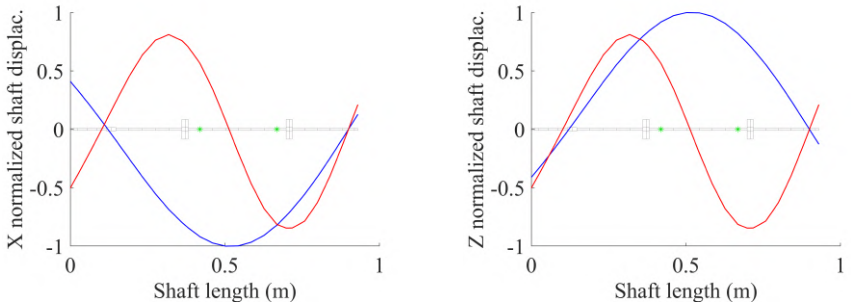

(a) (b)

Figure 4: Numerical Campbell Diagram

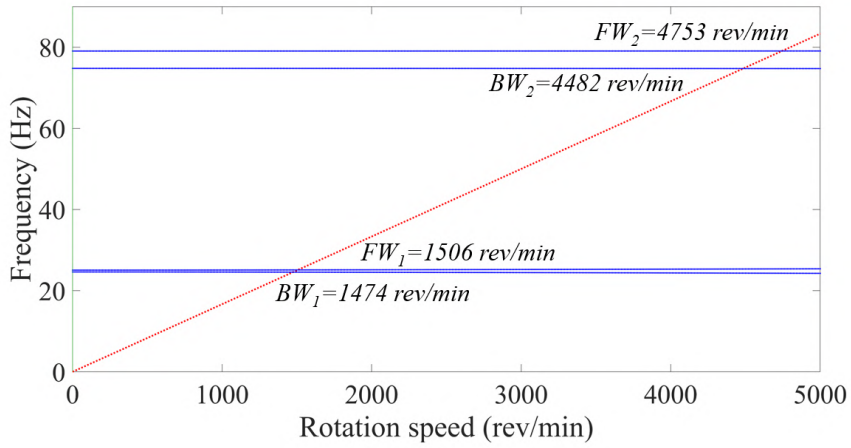

2.3 Electromagnetic Actuator (EMA)

Note by Fig. 1(a) that the rotor left bearing (B_1) is a hybrid bearing, meaning it is capable of both supporting and moving the shaft in order to control its vibrations.

The electromagnetic actuators are nothing more than electric coils, mounted in pairs on both horizontal and vertical directions. They are capable of applying only attraction forces on the shaft. Note that there are also four springs, which tend to linearize the EMA forces.

Each EMA is composed basically by a ferromagnetic body, which can be divided in two parts, according to Morais *et al.* (2013). The first one is the so-called core, which is an (E) shaped body, and receives the induction coil. The second one is the so-called target, which is an (I) shaped body, fixed to a roller bearing supporting the shaft, enabling the active control to be applied.

The EMA geometry is summarized in Fig 5.

Figure 5: EMA geometry.

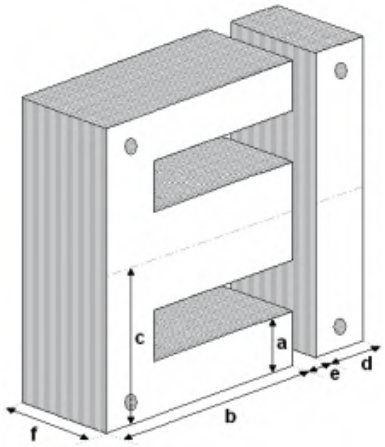

Table 2 presents physical parameters related to the EMAs used on the rotating machine hybrid bearing.

Table 2: Values of EMA geometrical parameters.

μ_o	$4\pi 10^{-7}\ (H/m)$
N	250 windings
a	$9.5\ mm$
b	$38.0\ mm$
c	$28.5\ mm$
d	$9.5\ mm$
e	$0.5\ mm$
f	$20.5\ mm$

The distance adjust between (E) and (I) parts was performed by a sliding apparatus. The distance between both parts is called *air gap*, or simply *gap*. In this work, the gap was set to be $500\mu m$ for all EMAs, what results in EMA attraction forces up to $150N$, making it possible to control the shaft lateral vibrations, according to Koroishi (2013). This distance was controlled by the use of mechanical fillers. Both (E) and (I) parts are composed by sets of insulated ferromagnetic sheets, for avoiding current losses (Foucault currents). According to Morais *et al.* (2013), the quality of the ferromagnetic circuit alloy is considered high enough and the nominal air gap between stator and beam is small enough so that the magnetic loss is considered negligible.

By the application of the good electrical currents, the EMA may compensate shaft vibrations causing them to decrease. The calculation of the good control currents and the decision of sending them on the right time is done by the active PID controller.

2.4 PID Active Controller

According to ADRIANO TESE, the PID technique is the most used for industry control applications, due to its efficiency and simplicity. Equation 2 presents the continuous PID control expression.

$$PID = \frac{K_T(K_D s^2 + K_P s + K_I)}{s} \tag{2}$$

where K_T stands for the total gain; K_D for the derivative gain; K_P for the proportional gain; and K_I for the integral gain.

Generally, the proportional gain affects mainly the system stiffness, since it multiplies the shaft displacements. Besides that, the derivative gain affects mainly the system damping, since it multiplies the shaft velocities. Finally, the integral

gain is devoted to suppress the steady state error, making the output to reach exactly the desired set point.

At this application, two different PID controllers were used for reducing the vibration amplitudes, (one for X and other for Z direction). The one for the X horizontal direction was tuned considering the gain values: $K_P = 7.5 \times 10^3$, $K_I = 0$, and $K_D = 20$. The other, designed for the Z vertical direction was tuned with the values: $K_P = 12.5 \times 10^3$, $K_I = 0$, and $K_D = 20$.

3. RESULTS

The numerical results are presented in this section, for $\omega = 1200$ rev/min, which represents a random operation speed. Besides that, and unbalance of $3.62x10^{-4}$ Kgm was applied, only to disc 1 (D_1).

It is worth mentioning how each EMA was numbered, according to Fig. 6. For suppressing shaft vibrations, the PID controller reads the displacement sensors S_{16_X} and S_{16_Z} (see Fig. 6) and based on their values, calculates the good current amplitudes for reducing shaft lateral vibrations.

This way, EMA#1 and EMA#3 are responsible for controlling vertical vibrations, based on sensor S_{16_Z} measurements. On the other hand, EMA#2 and EMA#4 are responsible for controlling horizontal vibrations, based on sensor S_{16_X} measurements.

Figure 6: Hybrid bearing with its EMA numbered

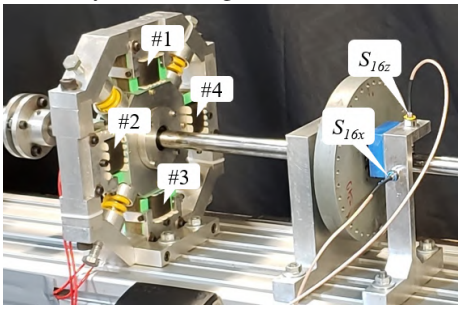

It is also important to mention that only the positive half of a sinusoidal current was used in each EMA. This was done for avoiding bias currents, what may increase EMA temperature in real applications. Besides that, each EMA is capable of applying only attraction forces.

The shaft lateral vibrations will be presented with and without the controller action. The chosen rotation speed for this paper was 1200 rpm. The motivation for choosing this rotating speed is because it does not have any relation with sub-harmonics of the first critical speed. For this reason, it would be a good candidate for real rotor operation speeds.

This way, Fig. 7 presents the PID controller result for $\omega = 1200$ rev/min. Note that the vibration amplitudes were considerably reduced for both vertical and horizontal directions. The non controlled displacements elliptic orbit presents a mean radius close to 94 μm, while the controlled one, has a mean radius around 38 μm.

Figure 7: PID controller result for $\omega_2 = 1200$ rev/min: Control Off (—), and Control On (—)

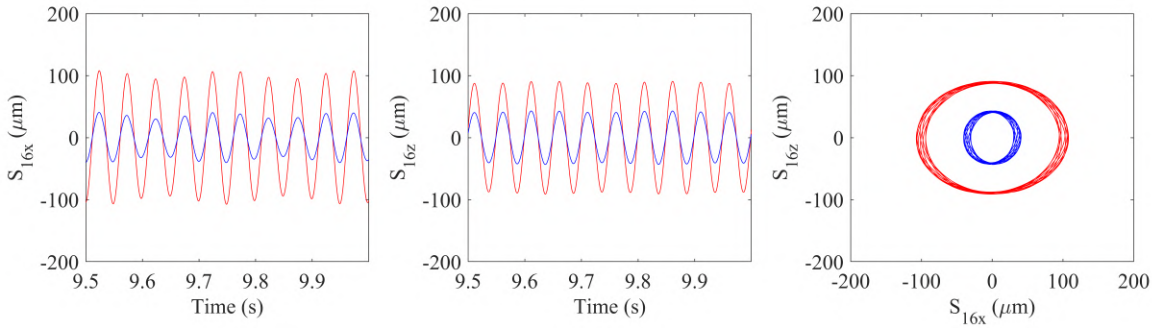

Is is important to measure the electrical currents derived by the PID controller for generating the active vibration control. Therefore, Fig. 8 presents the values, which are reasonably low, being completely capable of being applied on real electromagnetic actuators, with no danger of super-heating them. The analysis was performed on both horizontal and vertical directions, being depicted in Fig. 8(a) and Fig.8(b), respectively. This control current generation was done just like stated in the beginning of section 3by Fig. 6.

In a near future, an experimental validation will be performed, for the operation speed considered (1200 rev/min), since the present results are quite exciting.

Figure 8: Control Signals: (a) (—) EMA #2, (—) EMA #4 control currents, in mA and (—) S_{16_x} displacements, in μm; (a) (—) EMA #1, (—) EMA #3 control currents, in mA and (—) S_{16_z} displacements, in μm;

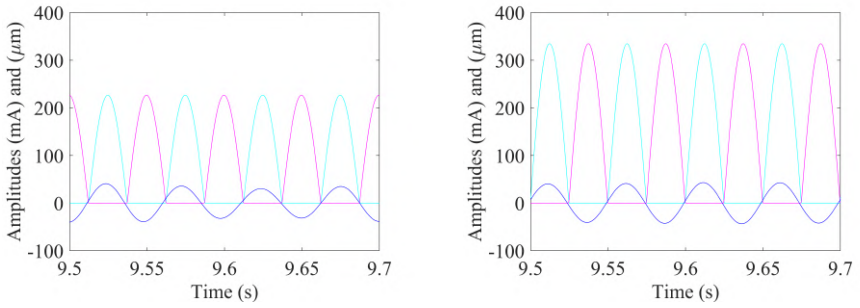

(a) (b)

4. CONCLUSIONS

This paper presented the results of a PID active controller, applied to an electromagnetic actuator (EMA), for reducing the lateral vibrations of a rotating machine. A FE numerical model was built and validated with the results of a real test rig. This way, one expects that this numerical model furnishes responses similar to the real test rig ones.

A PID active controller was used to derive the control currents that would cross each EMA, for reducing the vibration amplitudes of a rotating machine. The numerical results obtained highlight the efficiency of this technique, for reducing the shaft vibration amplitudes.

PID controllers are widely spread at the industrial context, due to both simplicity and efficiency. The quality of the numerical results obtained motivate experimental tests at the real test rig for facing out the numerical results just presented. It will be performed in a near future and more papers published in this context.

5. ACKNOWLEDGMENTS

The authors are thankful to the Brazilian Research Agencies FAPEMIG, CNPq (INCT-EIE) and also to CAPES for the financial support provided for this research effort.

6. REFERENCES

Cavalini-Jr, A.A., Lara-Molina, F.A., Dourado, A. and Steffen-Jr, V., 2015. "Fuzzy uncertainty analysis of a tilting-pad journal bearing". In *ASME 2015 International Design Engineering Technical Conferences and Computers and Information in Engineering Conference, Paper No. DETC2015-47586*.

Cavalini-Jr, A.A., Lobato, F.S., Koroishi, E.H. and Steffen-Jr, V., 2016. "Model updating of a rotating machine using the self-adaptive differential evolution algorithm". *Inverse Problems in Science and Engineering*, Vol. 24, pp. 504–523.

Koroishi, E.H., 2013. *Controle de Vibrações em Máquinas Rotativas utilizando Atuadores Eletromagnéticos*. Ph.D. thesis, Universidade Federal de Uberlânida.

Koroishi, E.H., Lara-Molina, F.A., Borges, A.S. and V. Steffen-Jr V Steffen, J., 2015. "Robust control in rotating machinery using linear matrix inequalities". *Journal of Vibration and Control*, Vol. 22, No. 17.

Lallane, M. and Ferraris, G., 1997. *Rotordynamics Prediction in Engineering*. John Wiley and Sons, 2nd edition.

Morais, T.S., Hogapian, D., Steffen-Jr, V. and Mahfoud, J., 2013. "Modeling and identification of electromagnetic actuator for the control of rotating machinery". *Shock and Vibration*, Vol. 20, pp. 171–179.

Nair, S.S., Vaidyan, M.V. and Joy, M.L., 2009. "Generalized design and disturbance analysis of robust h infinity control of active magnetic bearings". *2009 IEEE/ASME International Conference on Advanced Intelligent Mechatronics*.

Ogata, K., 2010. *Engenharia de Controle Moderno*. Pearson Prentice Hall, 5th edition.

Steffen-Jr, V., Rade, D.A. and Inman, D.J., 2000. "Using passive techniques for vibration damping in mechanical systems". *Journal of the Brazilian Society of Mechanical Sciences*, Vol. 22, No. 3.

Storn, R. and Price, K., 1995. "Differential evolution: A simple and efficient adaptative scheme for global optimization over continuous spaces". *International Computer Science Institute*, Vol. 12, No. 1, pp. 1–16.

7. INFORMATION RESPONSIBILITY

The authors are the only responsible for all the information included in this work.